Research Article

Journal of RAMAN SPECTROSCOPY

Received: 24 September 2009 Accepted: 8 November 2009

(wileyonlinelibrary.com) DOI 10.1002/jrs.2587

Single-beam coherent anti-Stokes Raman scattering (CARS) spectroscopy of gas-phase CO_2 via phase and polarization shaping of a broadband continuum

Sukesh Roy,[a]* Paul J. Wrzesinski,[b] Dmitry Pestov,[b] Marcos Dantus[b] and James R. Gord[c]

Coherent anti-Stokes Raman scattering (CARS) spectroscopy of gas-phase CO_2 is demonstrated using a single femtosecond (fs) laser beam. A shaped ultrashort laser pulse with a transform-limited temporal width of ∼7 fs and spectral bandwidth of ∼225 nm (∼3500 cm^{-1}) is employed for simultaneous excitation of the CO_2 Fermi dyads at ∼1285 and ∼1388 cm^{-1}. CARS signal intensities for the two Raman transitions and their ratio as a function of pressure are presented. The signal-to-noise ratio of the single beam–generated CO_2 CARS signal is sufficient to perform concentration measurements at a rate of 1 kHz. The implications of these experiments for measuring CO_2 concentrations and rapid pressure fluctuations in hypersonic and detonation-based chemically reacting flows are also discussed. Copyright © 2010 John Wiley & Sons, Ltd.

Keywords: Raman spectroscopy; femtosecond CARS; single-beam CARS; Fermi dyads; carbon dioxide; pulse shaping

Introduction

Evaluating the efficiency of combustion processes in hydrocarbon-fueled reacting flows requires accurate measurements of CO_2 concentration, both in the combustion zones and in the exhaust streams of propulsion and other engine systems.[1–4] Spatially and temporally resolved measurements of CO_2 concentration can provide valuable information regarding local combustion chemistry for real-time control of reacting-flow devices. Moreover, CO_2 is an important greenhouse gas, and along with CO, generally accounts for most of the carbon that is emitted from hydrocarbon-based reacting flows.[1,2] Because of the importance of CO_2 in gas-phase combustion chemistry, significant efforts based on diode lasers[3–5] and nanosecond (ns) lasers[6–10] have been made to measure the concentration of CO_2 in reacting flows and in engine exhaust streams using linear and nonlinear spectroscopic techniques. Most diode laser–based spectroscopic measurements rely on line-of-sight absorption spectroscopy and do not provide the spatial resolution necessary to monitor the local combustion chemistry for real-time control of combustion processes. The low repetition rates (typically 10–20 Hz) of nanosecond laser–based measurements are inadequate for addressing the transient phenomena associated with thermal and fluid-dynamic instabilities, generally ranging from 200 Hz to 10 kHz, although they do provide the required spatial resolution.[11,12]

Coherent anti-Stokes Raman scattering (CARS) spectroscopy is a very well-known spectroscopic tool for measuring gas-phase temperature and species concentration in reacting flows.[4,6–8,10] In CARS spectroscopy, the pump and Stokes beams create coherence in the medium which, when probed by another laser beam, generates a signal at a blue-shifted wavelength; this signal is known as the anti-Stokes signal. In a typical gas-phase CARS spectroscopy experiment, the pump, Stokes, and probe beams are arranged in BOXCARS fashion, with the phase-matching between the laser beams maintained in a crossed-beam geometry.[6] In high-pressure, turbulent reacting flows where rapid spatiotemporal variations of pressure and temperature are present, maintaining the spatial overlap between the laser beams becomes extremely challenging, if not impossible.[8,10] The objective of the present study is to demonstrate the feasibility of performing CARS spectroscopy–based CO_2 concentration measurements using a single, shaped 7-fs (femtosecond) laser pulse.

Recently, fs laser–based gas-phase CARS spectroscopy using the traditional crossed-beam geometry has been demonstrated for measuring temperature and various species concentrations in gas cells and reacting flows.[13–20] Femtosecond laser–based spectroscopy has an inherent advantage for the excitation of two-photon resonances since a large number of photon pairs within the broad spectral bandwidth(s) of the laser pulse(s) contribute to the excitation of the same transition.[16,21] It has been shown that a coherence close to the maximum value of 0.5 can be induced in the medium using fs pump and Stokes lasers.[21] The major advantages of fs-CARS for gas-phase spectroscopy with currently available laser sources are (1) the relative insensitivity of the signal to the local

---

* Correspondence to: Sukesh Roy, Spectral Energies, LLC, 5100 Springfield Street, Suite 301, Dayton, OH 45431, USA. E-mail: sroy@woh.rr.com

a Spectral Energies, LLC, Dayton, OH 45431, USA

b Department of Chemistry, Michigan State University, East Lansing, MI 48824, USA

c Air Force Research Laboratory, Propulsion Directorate, Wright-Patterson AFB, OH 45433, USA

collisional environment for pressures up to 20 bar and (2) the ability to make temperature and species-concentration measurements at rates of 1 kHz or greater. High data-acquisition rates are essential for addressing the instability phenomena associated with reacting flows in air-breathing propulsion and augmentor systems. The data-acquisition bandwidth of the fs-CARS system can be readily enhanced using ultrafast lasers with repetition rates >1 kHz and high-speed charge-coupled device (CCD) cameras with image intensifiers.

Performing CARS spectroscopy with only a single beam could greatly improve the potential for making species-concentration measurements in reacting flows with limited optical access and challenging optical conditions, such as jet propulsion systems or chemically harsh environments, where the presence of significant temperature gradients alters the spatial overlap among the various laser beams on a shot-to-shot basis.[8,10] In single-beam CARS spectroscopy, the bandwidth of the laser is chosen so that it exceeds the magnitude of the Raman shifts for the transitions of interest. The coherence induced by the pump and Stokes photons within the laser bandwidth is then probed by a portion of the same laser beam, as demonstrated by Oron *et al*.[22] Several more recent demonstrations of single-beam CARS spectroscopy for measuring various species concentrations have been reported.[23–29] Oron *et al*.[22] proposed a phase- and polarization-control scheme related to single-beam CARS spectroscopy for effectively suppressing the nonresonant background. In this approach, the probe field is divided into two halves; the phase of half of the field is set 180° with respect to the pump and Stokes fields, and the polarization of the probe field is set orthogonal to that of the pump and Stokes fields. It should be noted that all the laser fields contributing to the CARS signal generation are delivered by the same laser beam. These steps ensure that the probe field is not temporally overlapped with the pump and Stokes fields, and the polarization of most of the residual nonresonant signal is orthogonal to that of the resonant CARS signal. In addition to the phase- and polarization-control scheme proposed by Oron *et al*.[22] an interferometric scheme was demonstrated by Lim *et al*.[26,27] for enhancing the resonant signal intensity using the nonresonant signal as a local oscillator. In their approach, Lim *et al*. showed that the nonresonant signal, which is generally considered a hindrance in CARS spectroscopy, can be used to enhance the detection limit of the CARS technique. In another heterodyne detection scheme that was demonstrated by Vacano *et al*.[28] the blue part of the laser beam acts as a local oscillator; this scheme has been shown to increase the detection limit dramatically – even in the presence of significant depolarization. Single-beam CARS spectroscopy has also been demonstrated for stand-off detection of various chemicals and explosives.[23–25]

The majority of the research efforts described above targeted molecules with a vibrational wavenumber in the range 200–1100 cm^{-1}. However, Raman excitation of di- and triatomic gas-phase molecules such as N_2 ($\omega_v \sim 2330$ cm^{-1}) and CO_2 ($\omega_v \sim 1280$–1400 cm^{-1}) using a single laser beam could be challenging because of the large bandwidth required. We have recently demonstrated the utility of this approach for detecting gas-phase N_2 molecule.[30] In the present study, we explore the feasibility of performing single-shot CARS spectroscopy of CO_2 where the Fermi dyads of CO_2 at ∼1285 and ∼1388 cm^{-1} are simultaneously excited using a shaped 7-fs laser beam.[31–34] Moreover, the use of the CARS signal–intensity ratios between the bands of the Fermi dyads for measuring local pressure in dynamic, chemically reacting environments, such as pulsed-detonation engines (PDEs) or hypersonic flows, is also discussed.

Experimental

A schematic diagram of the instrument is shown in Fig. 1. An 80-MHz Ti : sapphire oscillator was used to seed a regenerative amplifier. The spectral bandwidth of the laser beam was ∼50 nm at full width at half maximum (FWHM). The beam was first steered into a reflective 4f pulse shaper with a 128-pixel phase-only spatial light modulator (SLM). This shaper was used to perform a multiphoton intrapulse interference phase scan (MIIPS) to correct for phase distortions introduced by the optics in the regenerative amplifier which followed and ensure transform-limited (TL) pulses at the amplifier output.[35] The amplified pulses had a spectral bandwidth of ∼28 nm (FWHM) and maximum energy of 1 mJ/pulse. The laser pulse energy was then attenuated to ∼350 µJ, and the beam was focused with a 1-m focal length curved mirror into a hollow waveguide (HWG), which is a 39-cm-long glass capillary with a core diameter of ∼300 µm filled with Ar at ∼2 bar, to broaden the spectral bandwidth of the laser pulse to ∼225 nm through self-phase modulation (SPM). A small amount of negative chirp was introduced using the grating compressor in the amplifier to optimize the continuum-generation process. The average power of the laser beam at the exit of the HWG was ∼210 mW. The beam was then recollimated and directed into a second pulse shaper. This shaper had a 640-pixel dual mask SLM (CRi SLM-640-D) and was used for two purposes: (1) to ensure delivery of TL pulses at the CARS probe volume through MIIPS measurements and (2) to provide additional phase and polarization control over the laser pulse spectrum for CARS spectroscopy as described by Oron *et al*.[22] The shaped pulses with an approximate energy of 3.7 µJ/pulse were directed into a pressurized gas cell containing CO_2 by using a curved mirror of focal length 75 cm. The diameter of the laser beam was ∼10 mm. The generated CARS signal was separated using a 650-nm short-pass filter and a calcite polarizing cube, with the transmission axis set perpendicular to the polarization of the excitation photons. The CARS signal was focused into a spectrograph using an achromatic lens of 10 cm focal length and was detected with a liquid nitrogen–cooled CCD camera. To ensure accurate pulse shaping, MIIPS compensation was performed at the target location, with one of the windows from the gas cell placed into the beam path. The obtained TL pulse duration, after dispersion compensation but prior to phase and polarization shaping, was ∼7 fs.

For single-beam spectrally resolved CARS measurements of gas-phase CO_2, both polarization and phase shaping of the generated broadband continuum were implemented, as outlined in Fig. 2. Note that the apparent amplitude modulation of the spectrum at the output of a hollow-core waveguide (and associated non-Gaussian shape of the spectrum) is a commonly observed phenomenon and is characteristic of the SPM process.[36,37] A particular spectral intensity profile is determined by many experimental parameters, including the gas used (Ar, Kr, etc.), gas pressure and/or the gas pumping scheme (statically filled vs differential pumping), input pulse energy and duration, waveguide diameter and length, etc. This dependence on multiple variables makes it difficult to reproduce the exact spectra from one instrument to another but also serves as a convenient means for adjusting the laser pulse parameters. For instance, Nisoli *et al*.[36] note that the amplitude modulation can be smoothed by increasing the group-velocity dispersion in the waveguide.

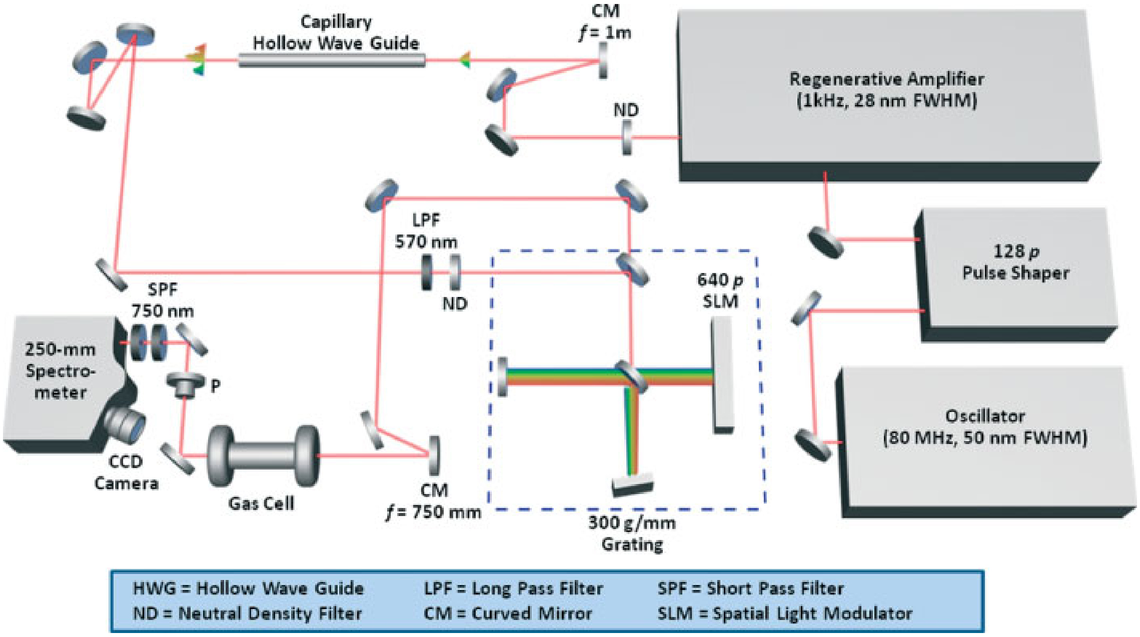

Figure 1. Schematic diagram of the single-beam CARS instrument for detection of gas-phase CO_2. HWG: hollow waveguide; CM: curved mirror; ND: neutral density filter; SPF: short-pass filter; LPF: long-pass filter; SLM: spatial light modulator; CCD: charge-coupled device.

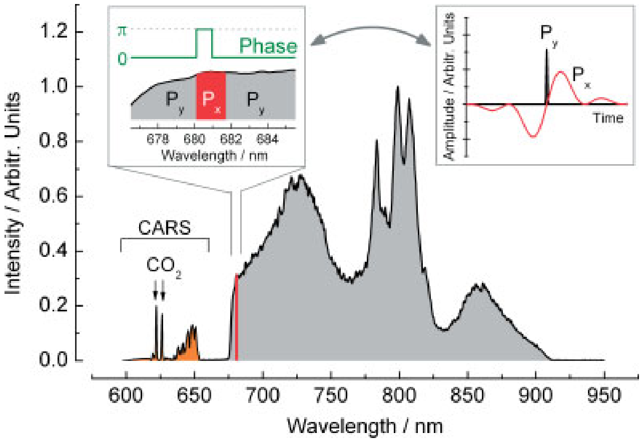

Figure 2. Phase and polarization shaping for single-beam CARS: spectra of the 7-fs laser pulse and CO_2 CARS signal. The normalized spectra of the incoming beam and collected CARS are not to scale. The *x*-polarized probe part of the laser spectrum covers four SLM pixels and is shown in red. CARS peaks corresponding to the Fermi resonances of CO_2 at ~1285 and ~1388 cm^{-1} are indicated by arrows. The left inset highlights the phase and polarization masks that are used (in conjunction with a polarizer placed after the gas cell) to gain the spectral resolution and suppress the nonresonant contribution; P_x and P_y refer to two mutually perpendicular linear polarizations. In the right inset, the temporal profiles of slowly varying field amplitudes for the orthogonally polarized excitation and probe parts of the laser pulse are sketched.

In our experiment, the spectral resolution was achieved by setting the polarization of a narrow strip of the laser spectrum (four SLM pixels wide at ~680 nm, 0.43 nm/pixel) at 90° with respect to the *y*-polarized laser spectrum and collecting only *x*-polarized CARS photons. Four pixels of the SLM correspond to a temporal width of ~2.1 ps. The observed Raman-resonant contribution to the scattered field is then dominated by an isotropic term that is proportional to the χ^{r}_{xxyy} element of the nonlinear optical susceptibility tensor, where the *x*-polarized band acts as a probe and the broadband *y*-polarized part of the spectrum impulsively excites molecular vibrations. Note that the nonresonant signal, in addition to χ^{nr}_{xxyy}, has a similar contribution from χ^{nr}_{xyyx} ($\chi^{nr}_{xxyy} = \chi^{nr}_{xyyx}$), where the *x*-polarized band acts as a pump.

The polarization-sensitive detection rejects the dominant but non-informative contribution from χ^{nr}_{yyyy} (and χ^{r}_{yyyy}). The remaining nonresonant background, passing through the polarizer, is further suppressed by phase shaping. Here, we program a π phase step at the central frequency of the probe band (left inset in Fig. 2); two of the four pixels are set to apply an additional π phase shift. In the time domain, this phase shift is equivalent to creating a node in the probe field at the moment of impulsive Raman excitation (right inset in Fig. 2), which effectively suppresses the nonresonant contribution.

Results and Discussion

An atmospheric-pressure, room-temperature single-beam spectrum of the Fermi dyads of CO_2 is shown in Fig. 3. The Fermi dyads appear because of the interaction of the Raman active symmetric stretch of CO_2 (1, 0°,0) with the overtone band of the infrared active bending mode (0,2°,0) coupled by the anharmonic part of the potential.[38,39] The energy levels associated with the Fermi resonance are then assigned as $(0,2^{\circ},0; 1,0^{\circ},0)_{I}$ and $(0,2^{\circ},0; 1,0^{\circ},0)_{II}$, where the subscript I refers to the higher energy state.[31,40] In Fig. 3, curves (A) and (B) denote the bands associated with the higher and lower energy states of the Fermi resonance, respectively. The spectrum shown in Fig. 3 was averaged over 10 laser shots, and the signal was attenuated by a neutral density filter with an optical density of ~2. The CARS signal was averaged to reduce shot-to-shot fluctuations arising mainly from nonlinearity in the HWG.

Although the statically filled HWG used in this work provides sufficiently large spectral bandwidth to impulsively excite the

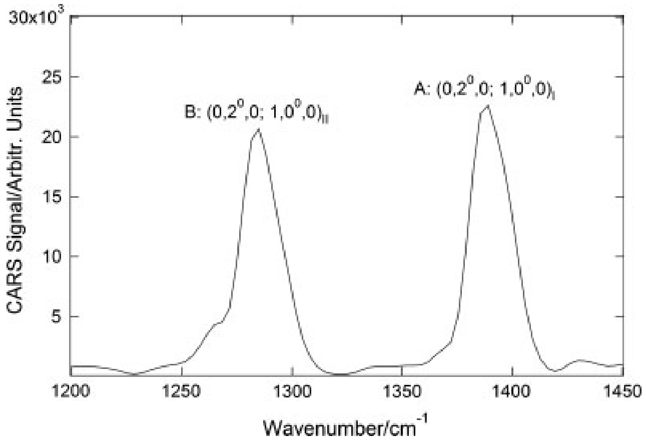

Figure 3. Single-beam CARS spectrum of atmospheric-pressure CO_2.

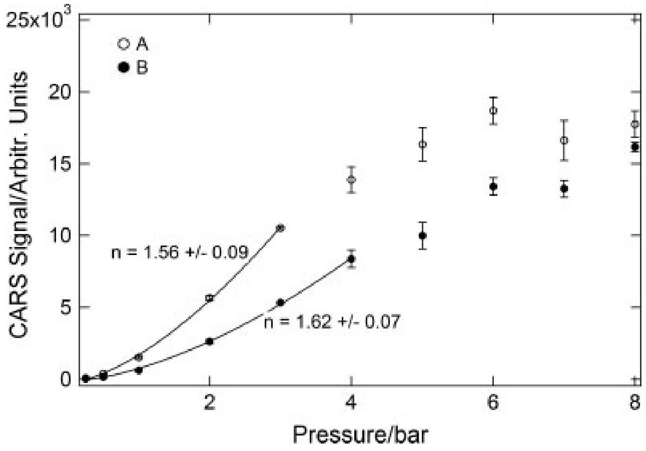

Figure 4. Single-beam CARS signal of CO_2 as a function of pressure. Symbols represent experimental data points; solid lines represent power curves fit through the data points obtained at pressures below 3 bar.

vibrational transitions of CO_2, this experimental approach suffers from large shot-to-shot pulse energy fluctuations. It was recently demonstrated that transitioning from a statically filled capillary to a differentially pumped one results in improved shot-to-shot stability.[37] Furthermore, improved energy conversion and increased broadening in the differentially pumped system have also been observed when compared to the statically filled HWG. Efforts are currently underway to incorporate these improvements in future experiments. It is clearly evident from Fig. 3 that the signal level of the CO_2 spectrum is sufficient to enable concentration measurements to be performed on a single-shot basis.

The dependence of the CO_2 CARS signal for bands A and B on gas pressure is shown in Fig. 4. It should be noted that at constant temperature, the number density of the gas molecules is directly proportional to the pressure since $n = p/k_BT$. Here, n is the number density; p, pressure; T, temperature; and k_B, the Boltzmann constant. Each data point represents the integrated intensity over the CARS spectrum shown in Fig. 3. It is observed for both transitions that the signal intensities do not depend on the square of the number density, as generally expected for CARS. Moreover, the signals reach a plateau after ~5 bar, indicating a level of saturation for the CARS signals. The saturation as well as the non-quadratic number–density dependence of the CARS signals may be due to (1) collisional line mixing and Dicke narrowing,[33] (2) effects of pressure on the coupling constant between the Fermi resonances,[41] and (3) saturation of the Raman transitions. A similar non-quadratic dependence of the CARS signal when using nanosecond lasers has been observed by Roh and Schreiber[42] and attributed to collisional mixing of various resonances and also to interference between the resonant and nonresonant signals; such interference should be minimal in the present experiment. Detailed modeling will be required to gain full understanding of the number–density dependence of the single-beam CO_2 CARS signals.

To investigate further the number–density dependence of the single-beam CO_2-CARS signal, measurements on bands A and B were performed for a mixture of CO_2 and Ar at 1 and 8 bar, as shown in Fig. 5(a) and (b), respectively. In this figure, the symbols represent experimental data points, and the solid curves are the result of power-law curve fitting through the points. For these experiments, the total gas pressure was maintained at a constant level, and the concentration of CO_2 and Ar was varied. It can be observed that the CARS signals display a nearly quadratic dependence on number density at 1 bar, whereas the exponents of the curves for the CARS signal *versus* number density are <1.5 at 8 bar. The non-quadratic dependence observed at 8 bar is similar to that observed by Roh and Schreiber[42] in ns-CARS experiments dominated by collisional mixing and narrowing. In the present experiment, even though the excitation process was initiated with a 7-fs laser beam, the coherence was probed with a ~2 ps probe field. It is possible that a few collisions might occur during the interaction process, thereby changing the quadratic dependence of the CO_2 CARS signal. We are currently developing a density matrix–based model for parametrically investigating the effects of collisions, Raman saturation, and the intensity of the laser fields on fs-CARS spectroscopy. Discussion of this modeling effort is beyond the scope of this paper.

Measurements were also performed to investigate the potential for applying the ratio of the integrated intensities for bands A and B to measure local pressure, in conjunction with CO_2 concentration measurements at rates of 1 kHz or greater, in dynamically changing environments, such as hypersonic or detonation-based chemically reacting flows.[43,44] Fig. 6 shows the ratio of integrated intensities of A (I_A) and B (I_B) as a function of pressure. It is observed that the ratio of I_A and I_B depends linearly on pressure. Similar behavior for the ratio of pure Raman signal intensities between A and B as a function of number density was observed for gaseous CO_2.[32,41] The ratio I_A/I_B changes with pressure because of the reduction of the Fermi resonance, which is caused by changes in the vibrational anharmonicity and enhanced repulsion of the vibrational levels.[41,45] Since the ratio I_A/I_B does not depend on temperature, its value reflects the local pressure at a particular instant.

Conclusions

Single-beam CARS spectroscopy of gaseous CO_2 with a ~7-fs shaped laser pulse has been demonstrated. It was confirmed that the bandwidth of the laser pulse was sufficient to create a strong coherence for molecules with vibrational wavenumbers >1100 cm^{-1}. In particular, CARS for CO_2 Fermi dyads at ~1285 and ~1388 cm^{-1} was observed. The signal-to-noise ratio of the CO_2 CARS spectrum was found to be sufficiently strong for performing single-shot measurements at a rate of 1 kHz or greater. The number–density dependence of the CARS signals

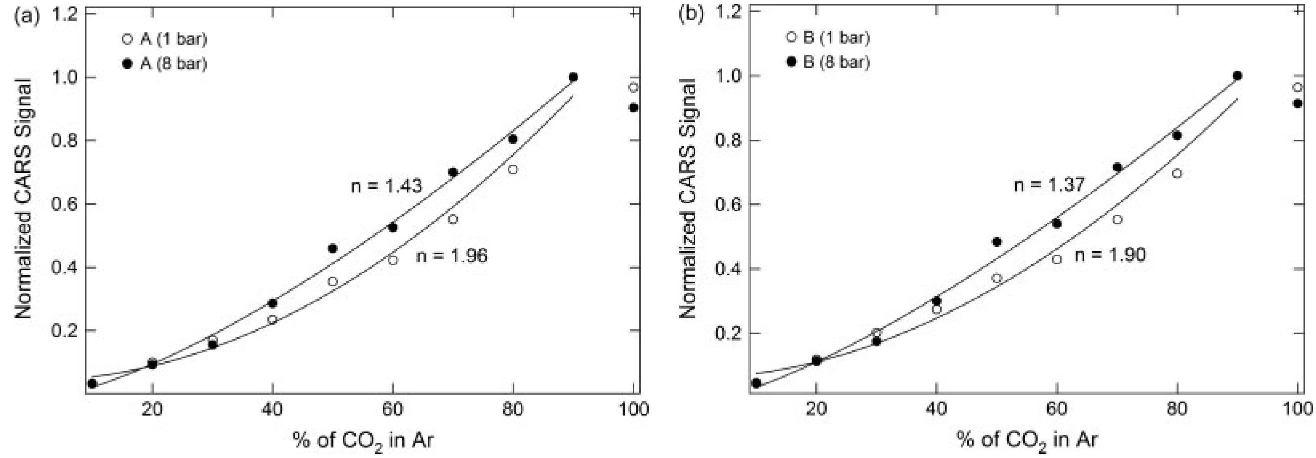

Figure 5. Femtosecond CARS signal of gas-phase CO_2 in mixtures with Ar at total cell pressures of 1 and 8 bar for transitions (a) A and (b) B. The solid lines represent the power curves fit through the data points.

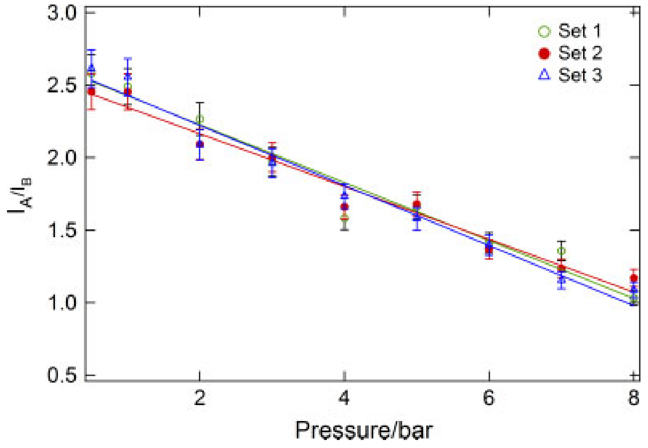

Figure 6. Ratio of integrated intensities of bands A and B as a function of gas pressure in pure CO_2. Three sets of data are presented to demonstrate the repeatability of the measurements.

displayed strong non-quadratic behavior, followed by saturation. We are currently designing various experiments to provide a full understanding of the fs-CARS signal dependence as a function of pressure. The integrated intensity ratios of the Fermi dyad bands as a function of pressure demonstrate that this approach could be used to measure local pressure in chemically dynamic environments, such as hypersonic or detonation-based chemically reacting flows.

Acknowledgements

Funding for this research was provided by the Air Force Research Laboratory under Phase II SBIR Contract No. FA8650-09-C-2918 (Ms Amy Lynch, Program Manager), by the AFRL Nanoenergetics Program, and by the Air Force Office of Scientific Research (Drs Julian Tishkoff and Tatjana Curcic, Program Managers).

References

[1] J. G. Canadell, C. Le Que’ re, M. R. Raupach, C. B. Field, E. T. Buitenhuis, P. Ciais, T. J. Conway, N. P. Gillett, R. A. Houghton, G. Marland, *Proc. Natl. Acad. Sci. U. S. A.* **2007**, *104*, 18866.
[2] P. Cox, C. Jones, *Science* **2008**, *321*, 1642.
[3] R. M. Mihalcea, D. S. Baer, R. K. Hanson, *Appl. Opt.* **1997**, *36*, 8745.
[4] M. E. Webber, J. Wang, S. T. Sanders, D. S. Baer, R. K. Hanson, In situ combustion measurements of CO, CO_2, H_2O and temperature using diode laser absorption sensors, *Proceedings of the Combustion Institute*, Edinburgh, Scotland, **2000**, *28*, 407.
[5] T. R. Meyer, S. Roy, T. N. Anderson, R. P. Lucht, R. Barron-Jimenez, J. R. Gord, *Opt. Lett.* **2005**, *30*, 3087.
[6] A. C. Eckbreth, *Laser Diagnostics for Combustion Temperature and Species*, (2nd edn), Gordon & Breach: The Netherlands, **1996**.
[7] M. Schenk, T. Seeger, A. Leipertz, *Appl. Opt.* **2005**, *44*, 6526.
[8] R. P. Lucht, V. Velur-Natarajan, C. D. Carter, K. D. Grinstead, J. R. Gord, P. M. Danehy, G. J. Fiechtner, R. L. Farrow, *AIAA J.* **2003**, *41*, 679.
[9] F. Vestin, K. Nilsson, P.-E. Bengtsson, *Appl. Opt.* **2008**, *47*, 1893.
[10] S. Roy, T. R. Meyer, R. P. Lucht, V. M. Belovich, E. Corporan, J. R. Gord, *Combust. Flame* **2004**, *138*, 273.
[11] G. A. Batley, A. C. McIntosh, J. Brindley, *Proc. R. Soc. London, A* **1996**, *452*, 199.
[12] W. Lee, J. G. Lee, D. A. Santavicca, *JSME Int. J. B* **2005**, *48*, 305.
[13] T. Lang, K.-L. Kompa, M. Motzkus, *Chem. Phys. Lett.* **1999**, *310*, 65.
[14] R. P. Lucht, S. Roy, T. R. Meyer, J. R. Gord, *Appl. Phys. Lett.* **2006**, *89*, 251112.
[15] J. R. Gord, T. R. Meyer, S. Roy, *Ann. Rev. Anal. Chem.* **2008**, *1*, 663.
[16] S. Roy, P. J. Kinnius, R. P. Lucht, J. R. Gord, *Opt. Commun.* **2008**, *281*, 319.
[17] S. Roy, D. Richardson, P. J. Kinnius, R. P. Lucht, J. R. Gord, *Appl. Phys. Lett.* **2009**, *94*, 144101.
[18] P. Beaud, H.-M. Frey, T. Lang, M. Motzkus, *Chem. Phys. Lett.* **2001**, *344*, 407.
[19] T. Lang, M. Motzkus, *J. Opt. Soc. Am. B* **2002**, *19*, 340.
[20] G. Knopp, P. Beaud, P. Radi, M. Tulej, B. Bougie, D. Cannavo, T. Gerber, *J. Raman Spectrosc.* **2002**, *33*, 861.
[21] R. P. Lucht, P. J. Kinnius, S. Roy, J. R. Gord, *J. Chem. Phys.* **2007**, *127*, 044316.
[22] D. Oron, N. Dudovich, Y. Silberberg, *Phys. Rev. Lett.* **2003**, *90*, 213902.
[23] O. Katz, A. Natan, Y. Silberberg, S. Rosenwaks, *Appl. Phys. Lett.* **2008**, *92*, 171116.
[24] H. Li, D. A. Harris, B. Xu, P. J. Wrzesinski, V. V. Lozovoy, M. Dantus, *Opt. Exp.* **2008**, *16*, 5499.
[25] H. Li, D. A. Harris, B. Xu, P. J. Wrzesinski, V. V. Lozovoy, M. Dantus, *Appl. Opt.* **2009**, *48*, B17.
[26] S.-H. Lim, A. G. Caster, S. R. Leone, *Phys. Rev. A* **2005**, *72*, 041803.
[27] S.-H. Lim, A. G. Caster, S. R. Leone, *Opt. Lett.* **2007**, *32*, 1332.
[28] Bv. Vacano, T. Buckup, M. Motzkus, *Opt. Lett.* **2006**, *31*, 2495.
[29] Bv. Vacano, W. Wohlleben, M. Motzkus, *J. Raman Spectrosc.* **2006**, *37*, 404.
[30] S. Roy, P. Wrzesinski, D. Pestov, T. Gunaratne, M. Dantus, J. R. Gord, *Appl. Phys. Lett.* **2009**, *95*, 074102.
[31] R. J. Blint, J. H. Bechtel, D. A. Stephenson, *J. Quant. Spectrosc. Radiat. Transfer* **1980**, *23*, 89.

[32] A. Hacura, *Phys. Lett. A* **1997**, *227*, 237.
[33] B. Lavorel, G. Millot, R. Saint-Loup, H. Berger, L. Bonamy, J. Bonamy, D. Robert, *J. Chem. Phys.* **1990**, *93*, 2185.
[34] R. B. Wright, C. H. Wang, *J. Chem. Phys.* **1973**, *58*, 2893.
[35] Y. Coello, V. V. Lozovoy, T. C. Gunaratne, B. Xu, I. Borukhovich, C.-H. Tseng, T. Weinacht, M. Dantus, *J. Opt. Soc. Am. B* **2008**, *25*, A140.
[36] M. Nisoli, S. D. Silvestri, O. Svelto, *Appl. Phys. Lett.* **1996**, *68*, 2793.
[37] J. S. Robinson, C. A. Haworth, H. Teng, R. A. Smith, J. P. Marangos, J. W. G. Tisch, *Appl. Phys. B: Lasers Opt.* **1996**, *85*, 525.
[38] P. E. Bernath, *Spectra of Atoms and Molecules*, (2nd edn), Oxford University Press: New York, **2005**.
[39] H. Olijnyk, H. Daufer, H.-J. Hodi, *J. Chem. Phys.* **1988**, *88*, 4204.
[40] R. Oberly, K. N. Rao, Y. H. Hahn, T. K. McCubbin, *J. Mol. Spectrosc.* **1968**, *25*, 138.
[41] A. Hacura, A. Brodka, L. Nikiel, F. G. Baglin, *J. Mol. Struct.* **1990**, *218*, 297.
[42] W. B. Roh, P. W. Schreiber, *Appl. Opt.* **1978**, *17*, 1418.
[43] S. T. Sanders, D. W. Mattison, L. Ma, J. B. Jeffries, R. K. Hanson, *Opt. Exp.* **2002**, *10*, 505.
[44] F. Schauer, R. Bradley, J. Hoke, Interaction of pulsed detonation engine with a turbine,*41st AIAA Aerospace Sciences Meeting & Exhibit*, Reno, NV, **2003**, 0891.
[45] C. H. Wang, R. B. Wright, *Chem. Phys. Lett.* **1973**, *23*, 241.